Optica Applicata, Vol. XLVIII, No. 2, 2018
DOI: 10.5277/oa180214

Truncated two-stage compound parabolic concentrator for collecting human diffuse transmission light

JING GAO[1*], GUANG HAN[2, 3], QIPENG LU[4], HAIQUAN DING[4], JIANGHONG XU[1], JIHAO SUN[1]

[1]College of Science, Yanshan University, Qinhuangdao, Hebei 066004, China

[2]Mechanical and Electrical Engineering Department,
Hebei Construction Material Vocational and Technical College,
Qinhuangdao, Hebei 066004, China

[3]College of Mechanical Engineering, Yanshan University,
Qinhuangdao, Hebei 066004, China

[4]State Key Laboratory of Applied Optics, Changchun Institute of Optics,
Fine Mechanics and Physics, Chinese Academy of Sciences,
Changchun, Jilin 130033, China

[*]Corresponding author: gaojing986@126.com

We propose an optical system employing a compound parabolic concentrator for near infrared spectroscope in noninvasive blood components testing. A truncated two-stage compound parabolic concentrator system is designed, which consists of a normal first-stage compound parabolic concentrator and a truncated second-stage compound parabolic concentrator. Using advanced ray tracing technique, the optical efficiencies of truncated two-stage compound parabolic concentrator system, ellipsoidal mirror system and non-optical-focusing mirror system are calculated to be 25.4%, 22.4% and 4.0%, respectively. Furthermore, the total length of truncated two-stage compound parabolic concentrator is only about 68 mm while the ellipsoidal mirror is 110 mm. It indicates that the truncated two-stage compound parabolic concentrator system enhances the ability of concentrating human diffuse transmission light, and it is a benefit to improve signal-to-noise ratio of noninvasive biochemical analysis system efficiently. Due to the advantage of small size, it tends to achieve a miniature instrument.

Keywords: optical design, compound parabolic concentrator (CPC), non-imaging optics, near infrared spectroscopy, medicine optical instrument.

1. Introduction

Blood components analysis is one of the basic methods of health diagnosis. For example, the current invasive method makes it difficult to perform frequent blood glucose measurements and keep better control of glucose level, which is crucial in reducing

the risk of complications. Near infrared (NIR) spectroscopy is a noninvasive, fast, multicomponent analysis technique and does not require sample preparations or reagents. In 1991, NORRIS reported possible medical applications of NIR in the 4th International Conference of NIR Spectroscopy [1]. After years of research and development, NIR spectroscopy has been extensively employed in the fields of agriculture, food, medicine, *etc*. [2–4]. Because of special advantages, it becomes one of the most promising approaches to realize noninvasive blood components analysis [5, 6]. When near infrared light incidents on human body, the light is partially absorbed and scattered, according to its interaction with chemical components in the blood, before transmitting to a detector. The transmission spectra contain the spectral signatures of blood components such as water, fat, glucose, hemoglobin, *etc*. Although numerous studies have been conducted, there is still a long way for the noninvasive clinical application. Complex interferences from skin tissue and weak valid spectral signal discourage the development of NIR noninvasive measurement [7–9]. For the second difficulty, the reason is that water absorption to light is very strong leading to serious light attenuation, and the contents of blood components are lower. Therefore, a high signal-to-noise ratio (SNR) spectroscope for measuring the blood components precisely and reliably is needed [7, 10].

The spectral SNR is proportional to the optical throughput Φ, the optical transmission efficiency ζ, and the square root of the number of collected and averaged spectral data for each spectral element $N^{1/2}$ [7]

$$\mathrm{SNR} \propto \Phi \zeta N^{1/2} \tag{1}$$

The optical throughput Φ is defined as

$$\mathrm{d}\Phi = I \mathrm{d}\Omega \tag{2}$$

where I is light intensity and Ω is solid angle. Combing Eqs. (1) and (2), we obtain that SNR is proportional to light intensity. Thus, SNR can be improved by increasing the luminance of source or optical efficiency of apparatus. The improvement of the luminance of source is limited, while there are more applications of the second method. HAI-BO LIU *et al*. used a THz time-domain spectroscopy system in combination with a diffuse reflectance accessory to acquire the reflection spectrum of the explosive RDX (hexahydro-1,3,5-trinitro-1,3,5-triazine) [11]. In the diffuse reflectance accessory, the THz beam was focused on the sample by an off-axis ellipsoidal mirror, and then a quarter of the diffusely reflected radiation was collected by the second off-axis ellipsoidal mirror. VAN DER MARK and DESJARDINS proposed to use broadband light that was spectrally dispersed, coded and recombined before being delivered to the tissue [12]. In this method, light from the tissue can be detected with a high numerical aperture photodetector and then spectrally demodulated. MARUO *et al*. assembled a double-beam type of spectrometer with a unique optical fiber probe for noninvasive blood glucose measurements [13]. The probe consisted of twelve separated source optical fibers and one detector optical fiber. This optical fiber not only transmitted light but also was used

as a device of collecting human diffuse transmission light. Although this optical geometry enabled the selective measurement of dermis tissue spectra, the spectral signal received by detector is weak. In 1978, a compound parabolic concentrator (CPC) was first invented by WELFORD and WINSTON to concentrate the solar radiation on a small area [14]. Up to now, CPC has been widely used in applications such as collecting solar radiation, concentrating feeble scattering light and photovoltaic applications [14–17]. The light entering CPC over the large aperture within a small solid angle is concentrated into the small aperture. In this paper, we specifically focus our interest on building an optical system which can collect human diffuse transmission light onto detector efficiently. This configuration having high optical efficiency increases the optical throughput. According to Eq. (1), it is conducive to the improvement of SNR, and to further increase in the precision of the noninvasive biochemical measurement system.

Based on the optical principle of CPC, we present a two-stage compound parabolic concentrator (TCPC) system. Utilizing a ray tracing technique, the configuration is confirmed to have superior optical performance when the first-stage CPC is normal and the second-stage CPC is truncated. Without considering the optical properties of skin tissue, truncated TCPC system, ellipsoidal mirror system and non-optical-focusing-mirror system are compared and the results are discussed.

2. CPC geometry

CPC consisting of two halves of parabolas is a non-imaging concentrator based on the marginal optical principle. The geometry of CPC is shown in Fig. 1. Parabola A and parabola B are symmetric with respect to y-axis. F_2 and F_1 are the focal points of parabola A and parabola B, respectively. NF_1 and MF_2 are parallel to the axes of parabola A and parabola B, respectively; the angle between NF_1 and MF_2 is $2\theta_a$, and θ_a is called an acceptance half-angle.

If the incident angle θ satisfies $\theta \leq \theta_a$, the light entering CPC at large aperture (entrance plane) will be reflected once by the inner surface before exiting CPC at small

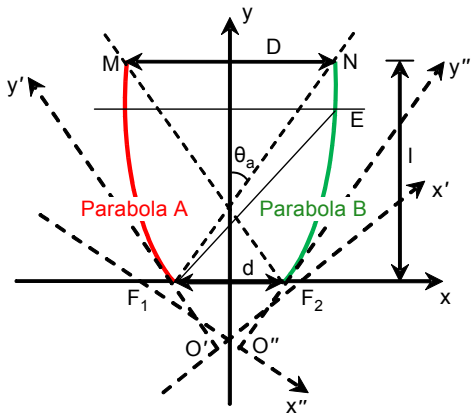

Fig. 1. Geometry of CPC.

aperture (exit plane). On the contrary, the light will be reflected first above the focus and then exit CPC at large aperture suffering several reflections. Only the portion within the acceptance half-angle θ_a can be collected.

In Fig. 1, the equations of parabola A and parabola B respectively can be expressed in the following forms:

$$\left[\sqrt{df-f^2}\,x-\left(f-\frac{d}{2}\right)y\right]^2-df^2x-d\left(f+\frac{d}{2}\right)\sqrt{df-f^2}\,y=\frac{fd^2(f+d)}{4} \tag{3}$$

$$\left[\sqrt{df-f^2}\,x+\left(f-\frac{d}{2}\right)y\right]^2+df^2x-d\left(f+\frac{d}{2}\right)\sqrt{df-f^2}\,y=\frac{fd^2(f+d)}{4} \tag{4}$$

where d is the diameter of small aperture, f is the focal length of parabola. Assuming that O′ is the intersection point of extended line and axis of parabola B, O″ is the intersection point of extended line and axis of parabola A, we have

$$f=\left|\mathrm{O'F_1}\right|=\left|\mathrm{O''F_2}\right|=\frac{d(1+\sin(\theta_a))}{2} \tag{5}$$

If the acceptance half-angle θ_a and the small aperture diameter d are known, the shape of CPC can be generated. The diameter of large aperture (represented by D) and the length (represented by l) of CPC are written as

$$D=\frac{d}{\sin(\theta_a)},\qquad l=\frac{D+d}{2}\cot(\theta_a) \tag{6}$$

The geometric concentration ratio of CPC is related to the acceptance half-angle,

$$C=\frac{D}{d}=\frac{1}{\sin(\theta_a)} \tag{7}$$

According to Eqs. (6) and (7), the focusing performance could be improved by decreasing θ_a, but the larger D and l are leading to a larger CPC. It will certainly be a hindrance to acquire miniature instrument.

3. Optical design

The schematic of a near infrared spectral noninvasive measurement system is shown in Fig. 2. This system consists of 75 W halogen tungsten lamp from 780 to 2500 nm, convergent lens, rotating plate with eight filters (∅20 mm) of different wavelengths, TCPC system, G8605-15 InGaAs PIN photodiode detector of Hamamatsu Photonics Co. with photosensitive area ∅5 mm, pretreatment circuit including two stages amplifying circuit with AD549J operational amplifier and filter circuit, 6281 M multi-function

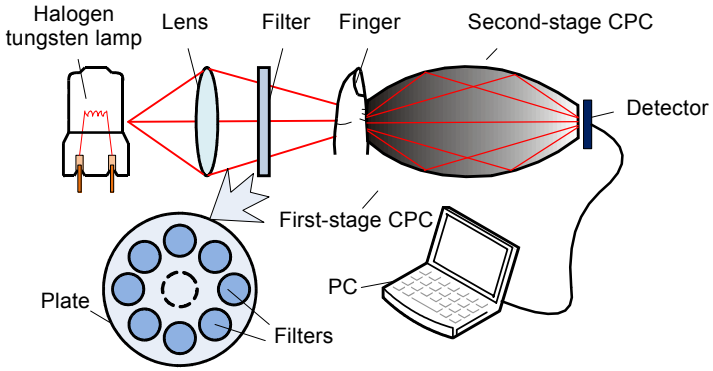

Fig. 2. Schematic diagram of near infrared spectra measurement by using transmittance mode.

data acquisition card and spectral analysis software TQ Analyst. We select 6281 M data acquisition card which is produced from National Instruments whose maximum conversion resolution is 18 bits, sample rate is 625 kS/s and common-mode rejection ratio is 110 dB. TQ Analyst is a commonly used spectral analysis software, and it can provide various qualitative and quantitative analysis tools applied in mid-infrared, near infrared, far infrared and Raman spectroscopy.

In TCPC system, the first-stage CPC can decrease the divergent angle of diffuse light; the second-stage CPC can further concentrate diffuse light onto the detector. In the following optical calculations, we use the software TracePro as an assistant analysis tool.

3.1. Establishment of the first-stage CPC

The structure parameters of the first-stage CPC and the second-stage CPC are denoted by d_1, D_1, θ_{1a}, d_2, D_2, θ_{2a}, respectively, and the values of D_1 and D_2 are equal. The part of the tested finger is defined to be a circle with a diameter d_1 = 10 mm. Moreover, the overall length of TCPC system is less than 110 mm. For convenience of TCPC de-

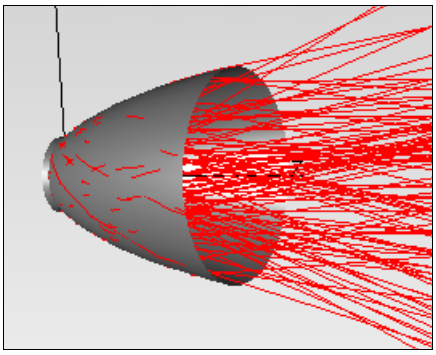

Fig. 3. Rays reflected by the first-stage CPC.

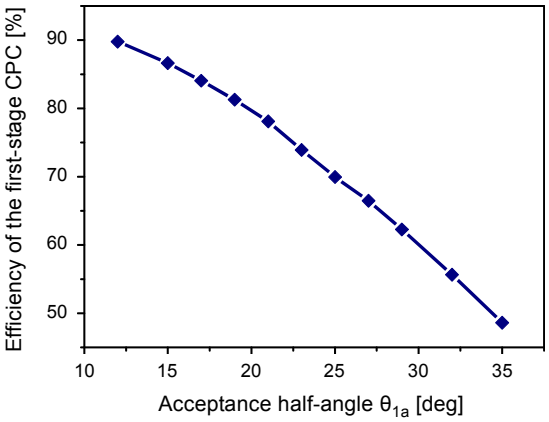

Fig. 4. Efficiency of the first-stage CPC with different acceptance half-angles and d_1 = 10 mm.

sign, we suppose that the measured part of human body is Lambertian radiation surface source. When diffuse light emitted from it is reflected by the first-stage CPC (see Fig. 3), the ratio of the power of reflected light, for the angle not greater than the acceptance half-angle θ_{1a}, to the power of incident light, *i.e.*, the efficiency of the first -stage CPC is calculated, as shown in Fig. 4.

Figure 4 illustrates that the efficiency of the first-stage CPC decreases with the increase in the acceptance half-angle θ_{1a}. It can be inferred that the low efficiency of large acceptance half-angle is due to the small geometric concentration ratio. However, the length of the first-stage CPC increases with the decrease in the field of view. If the efficiency is limited to be not less than 70%, θ_{1a} is not larger than 25°. Because of the overall length of TCPC not beyond 110 mm, the length of the first-stage CPC is considered to be not more than 55 mm, and then θ_{1a} is not smaller than 20°. Therefore, the range of θ_{1a} is changed from 20° to 25°.

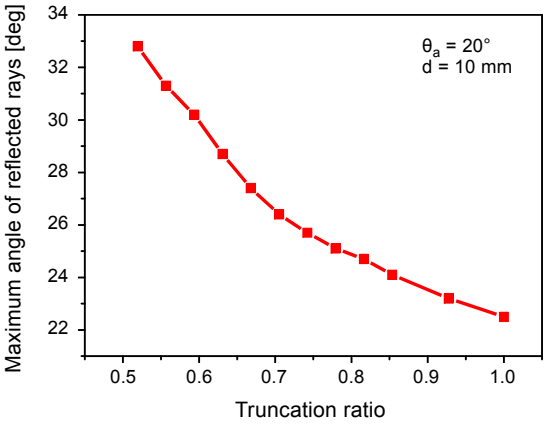

Fig. 5. Variation of the maximum angle of rays reflected by truncated CPC with θ_a = 20° and d = 10 mm.

Although CPC with small θ_a has well focusing characteristics, the length is large. For this reason, the truncation method [18–20] is applied to reduce the length of CPC. Meanwhile, the large aperture of truncated CPC fits in with the other normal one. Truncation ratio is calculated as the ratio of the length after truncation to the original length.

Figure 5 shows the variation of the maximum angle of rays reflected by truncated CPC with $\theta_a = 20°$ and $d = 10$ mm. From Fig. 5, the maximum angle of rays reflected by truncated CPC decreases with the increase in the truncation ratio. Therefore, the first-stage CPC is designed in normal structure, which reduces the angle of reflected light.

3.2. Establishment of the second-stage CPC

Suppose the incident angle is θ, θ_t is the angle between the ray from the edge E of the truncated large aperture to the edge F_1 of the small aperture (see Figs. 1 and 6), then angular acceptance function $F(\theta)$ is considered to be the ratio of the number of received

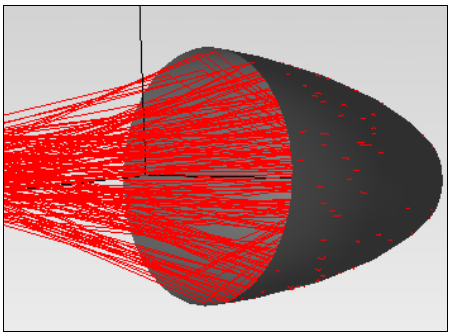

Fig. 6. Rays reflected by the second-stage CPC.

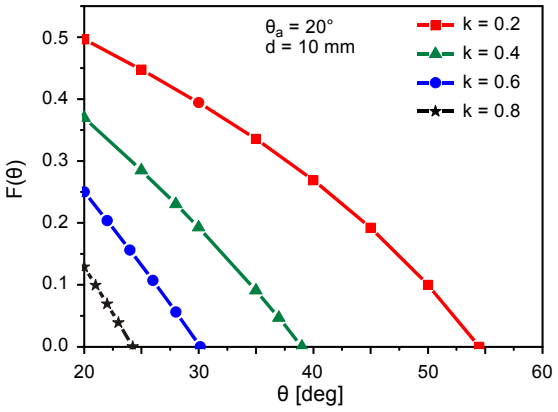

Fig. 7. Angular acceptance function $F(\theta)$ for truncated CPC with $\theta_a = 20°$, $d = 10$ mm, and $k = 0.2$, 0.4, 0.6, and 0.8.

rays to the number of incident rays. Using the equations for parabola and performing some algebra, $F(\theta)$ is expressed as follows [21]:

$$F(\theta) = \begin{cases} 1, & \theta \le \theta_a \\ \dfrac{1+C}{2C}\left(1 - \dfrac{\tan(\theta)}{\tan(\theta_t)}\right), & \theta_a < \theta \le \theta_t \\ 0, & \theta > \theta_t \end{cases} \tag{8}$$

In Fig. 7, we show the result of $F(\theta)$ for truncated CPC with $\theta_a = 20°$, $d = 10$ mm and truncation ratio k from 0.2 to 0.8. It is clear from Eq. (8) and Fig. 7 that truncated CPC can accept light whose angle is greater than θ_a compared with normal CPC. Besides, the CPC with small truncation ratio is conducive to acceptance of the light with large angle. Therefore, it is better that the second-stage CPC is chosen to be truncated structure.

3.3. Calculation of truncated TCPC

The results in Sections 3.1 and 3.2 serve as the basis for design of truncated TCPC consisting of a normal first-stage CPC and a truncated second-stage CPC. Figure 8 shows variation of optical efficiency for different configurations where each figure compares different acceptance half-angles.

In Fig. 8, the second-stage CPC with $d_2 = 9$ mm performs higher optical efficiency than the CPC with $d_2 = 10$ mm, and truncated TCPC with large acceptance half -angle θ_{2a} has better optical performance. That is because it allows some rays beyond the normal acceptance half-angle to reach the small aperture. Moreover, small acceptance half-angle θ_{1a} of first-stage CPC reduces the angle of diffuse light and increases the diameter of large aperture, hindering the truncation of second-stage CPC. There-

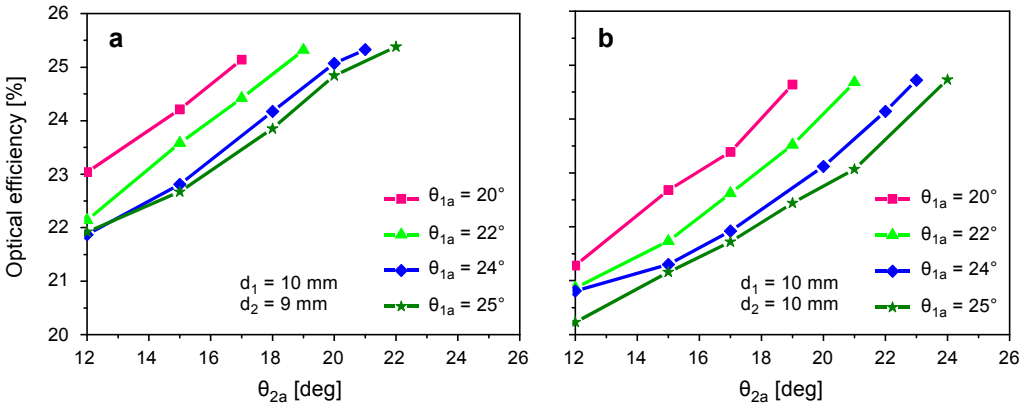

Fig. 8. Variation of optical efficiency for different truncated TCPC consisting of normal first-stage CPC and truncated second-stage CPC; $d_2 = 9$ mm (**a**) and $d_2 = 10$ mm (**b**).

fore, the optimized parameters are as follows: $d_1 = 10$ mm, $\theta_{1a} = 25°$, $d_2 = 9$ mm, and $\theta_{2a} = 22°$. In this configuration, the optical efficiency is about 25.4%, and the total length is only about 68 mm.

In the previous research, we obtained the best ellipsoidal mirror in which the length of major axis is 140 mm, and the distance between two focus points is 110 mm [22]. In this system, the measured part and detector are positioned at two focus points, respectively. Sometimes, the human diffuse transmission light is directly received by detector without focusing accessory in infrared spectroscopy instrument. We suppose the distance between the measured part and the detector tilted 45° is 10 mm in the non-optical -focusing mirror system. The optical efficiency of the ellipsoidal mirror system is calculated to be 22.4% and the optical system without the focusing mirror is only 4.0%. The rays' irradiance distributions of these three structures on the detector are shown in Fig. 9. We see the use of truncated TCPC can keep the optical efficiency at a satisfactory level with a small dimension, and make the light irradiate on the detector evenly.

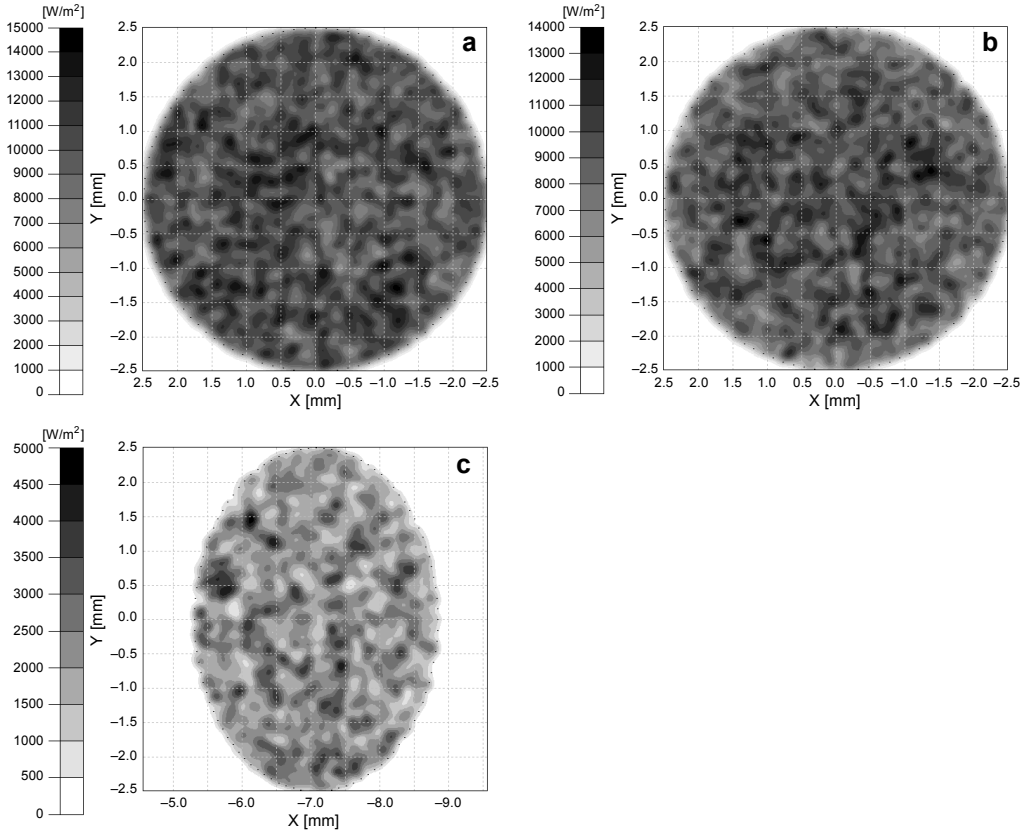

Fig. 9. Irradiance map. Truncated TCPC system (**a**), ellipsoidal mirror system (**b**), and non-optical -focusing mirror system (**c**).

4. Conclusions

In this paper, we propose a truncated TCPC system based on the characteristics of CPC. This truncated TCPC system consists of a normal first-stage CPC and a truncated second-stage CPC. Its optical performance optimization is discussed in terms of the normal first-stage CPC parameters variations and different truncated second-stage CPC configurations. By changing the aperture's diameter, acceptance half-angle and truncation ratio, we realize a high optical efficiency system. Comparisons with the ellipsoidal mirror system and the non-optical-focusing mirror system confirm that the truncated TCPC system can concentrate diffuse transmission light from the measured part onto the detector effectively. Therefore, the optical throughput from the measured part to detector is improved. According to Eq. (1), we know that it can improve SNR of the system effectively, providing support for accurate analysis of blood components. Besides, the new structure is small in size tending to achieve miniature instrument. In the next step, we will enhance the level of this truncated TCPC and do some experiments.

Acknowledgments – The authors would like to acknowledge the financial support from Science and Technology Research Project of University of Hebei Province (Grant No. Z2017002), National Natural Science Foundation of China (Grant Nos. 61308067 and 61475155).

References

[1] NORRIS K., *Possible Medical Applications of NIR, Making Light Work: Advances in Near Infrared Spectroscopy*, Ian Michael Publication, Aberdeen, 1992, pp. 596–602.

[2] HUAIPU SONG, DELWICHE S., YUD-REN CHEN, *Neural network classification of wheat using single kernel near-infrared transmittance spectra*, Optical Engineering 34(10), 1995, pp. 2927–2934.

[3] OEMRAWSINGH R.M., CHENG J.M., GARCÍA-GARCÍA H.M., VAN GEUNS R.-J., DE BOER S.P.M., SIMSEK C., KARDYS I., LENZEN M.J., VAN DOMBURG R.T., REGAR E., SERRUYS P.W., AKKERHUIS K.M., BOERSMA E., *Near-infrared spectroscopy predicts cardiovascular outcome in patients with coronary artery disease*, Journal of the American College of Cardiology (JACC) 64(23), 2014, pp. 2510–2518.

[4] PAL S., PRAJAPATI Y.K., SAINI J.P., SINGH V., *Sensitivity enhancement of metamaterial-based surface plasmon resonance biosensor for near infrared*, Optica Applicata 46(1), 2016, pp. 131–143.

[5] SHINDE A.A., PRASAD R.K., *Non invasive blood glucose measurement using NIR technique based on occlusion spectroscopy*, International Journal of Engineering Science and Technology **3**(12), 2011, pp. 8325–8333.

[6] ZHEN-HAO HUANG, CHANG-NING HAO, LIN-LIN ZHANG, YAN-CHAO HUANG, YI-QIN SHI, GENG-RU JIANG, JUN-LI DUAN, *Non-invasive blood glucose sensing on human body with near-infrared reflection spectroscopy*, Proceedings of SPIE 8193, 2011, article ID 81931O.

[7] SAPTARI V.A., *A Spectroscopic System for Near Infrared Glucose Measurement*, Ph.D. Thesis, Massachusetts Institute of Technology, Massachusetts, 2004.

[8] PICKUP J.C., HUSSAIN F., EVANS N.D., SACHEDINA N., *In vivo glucose monitoring: the clinical reality and the promise*, Biosensors and Bioelectronics 20(10), 2005, pp. 1897–1902.

[9] KRAMER K.E., *Improving the Robustness of Multivariate Calibration Models for the Determination of Glucose by Near-Infrared Spectroscopy*, Ph.D. Thesis, University of Iowa, Iowa, 2005.

[10] Rong Liu, Bin Deng, Wenliang Chen, Kexin Xu, *Next step of non-invasive glucose monitor by NIR technique from the well controlled measuring condition and results*, Optical and Quantum Electronics 37(13–15), 2005, pp. 1305–1317.

[11] Hai-Bo Liu, Yunqing Chen, Bastiaans G.J., Zhang X.-C., *Detection and identification of explosive RDX by THz diffuse reflection spectroscopy*, Optics Express 14(1), 2006, pp. 415–423.

[12] Van der Mark M.B., Desjardins A., *Diffuse spectroscopy with very high collection efficiency*, CLEO: 2011 – Laser Applications to Photonic Applications, OSA Technical Digest (CD), Optical Society of America, 2011, article ID ATuB4.

[13] Maruo K., Tsurugi M., Tamura M., Ozaki Y., *In vivo noninvasive measurement of blood glucose by near-infrared diffuse-reflectance spectroscopy*, Applied Spectroscopy **57**(10), 2003, pp. 1236–1244.

[14] Welford W.T., Winston R., *The Optics of Nonimaging Concentrators: Light and Solar Energy*, Academic Press, New York, 1978.

[15] Jingyue Fang, Hailiang Zhang, Honghui Jia, Hongwei Yin, Shengli Chang, Shiqiao Qin, *Compound parabolic concentrator applied as receiving antenna in scattering optical communication*, Chinese Optics Letters **8**(5), 2010, pp. 478–481.

[16] Winston R., *Thermodynamically efficient solar concentrators*, Journal of Photonics for Energy 2(1), 2012, article ID 025501.

[17] Siti Hawa Abu-Bakar, Firdaus Muhammad-Sukki, Roberto Ramirez-Iniguez, Tapas Kumar Mallick, Abu Bakar Munir, Siti Hajar Mohd Yasin, Ruzairi Abdul Rahim, *Rotationally asymmetrical compound parabolic concentrator for concentrating photovoltaic applications*, Applied Energy 136, 2014, pp. 363–372.

[18] Tripanagnostopoulos Y., Yianoulis P., Papaefthimiou S., Zafeiratos S., *CPC solar collectors with flat bifacial absorbers*, Solar Energy 69(3), 2000, pp. 191–203.

[19] Segal A., Epstein M., *Truncation of the secondary concentrator (CPC) between maximum performances and economical requirements*, Proceedings of SPIE 7423, 2009, article ID 74230H.

[20] Leonardi E., *Detailed analysis of the solar power collected in a beam-down central receiver system*, Solar Energy 86(2), 2012, pp. 734–745.

[21] Carvalho M.J., Collares-Pereira M., Gordon J.M., Rabl A., *Truncation of CPC solar collectors and its effect on energy collection*, Solar Energy 35(5), 1985, pp. 393–399.

[22] Gao Jing, Lu Qipeng, Peng Zhongqi, Ding Haiquan, *Parameter design and optimization of collecting light ellipsoidal reflector in near infrared noninvasive biochemical analysis*, Acta Physica Sinica 32(8), 2012, article ID 0822007.

Received April 11, 2017
in revised form June 10, 2017